Sensor for the Control and Damping of 'Violin-Mode' Resonances in Silica suspension Fibres

N.A. Lockerbie and K.V. Tokmakov
SUPA, University of Strathclyde, Glasgow, Scotland, UK

Concept of shadow sensor

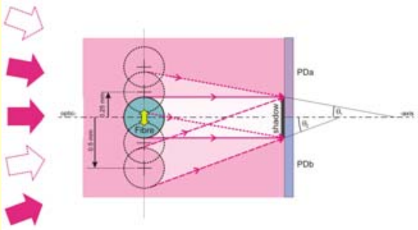

Figure 1. Plan view of cylindrical silica suspension and dual-photodiode shadow-sensor. Violin-Mode (VM) resonance detection (double-headed arrow) and 'creep' compensation (dashed-circles): see text.

In Fig.1 Violin-Mode (VM) resonance, and 'creep', in a silica suspension fibre, is indicated by the double-headed arrow, and the dashed-circles, respectively. The VM vibration is detected using a shadow sensor comprising photodiodes PDa and PDb. A CW infrared beam (890 nm) can be switched on at one of five different angles of incidence, to compensate for any creep in the fibre's position, such that the fibre's shadow always overlaps both detectors. The differential photocurrent from these detectors constitutes the 'Violin-Mode' signal.

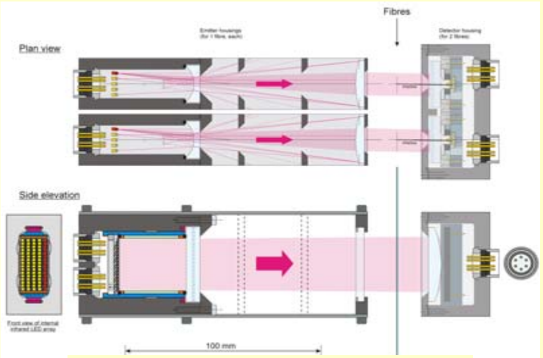

Figure 2. Violin-Mode detection system for two suspension fibres.

In Fig.2 two separate emitters and two dual split-photodiode detectors (the latter in a single housing) are shown. Each emitter comprises five columns of 16 x OP224 infrared LEDs, in a reversed Galilean telescopic optical arrangement (using cylindrical lenses).

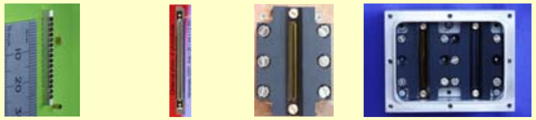

Column of LEDs. Single Photodiode. Split-photodiode with 90° prism. Dual split-photodiode detector housing

Figure 3. Infrared LED source and split-photodiode detector system.

Figs.3, 4, and 5 show the component parts of the VM detection system. Fig.6 shows the VM emitter / detector control system for all four fibres of a suspension system. Figs. 7 and 8 show the modulated infrared method used to obtain the VM amplifier's (Fig.9) bandwidth—Fig.10. Fig.11 shows the amplifier's noise performance, whilst Fig.12 shows the system's *DC* sensitivity to shadow displacement.

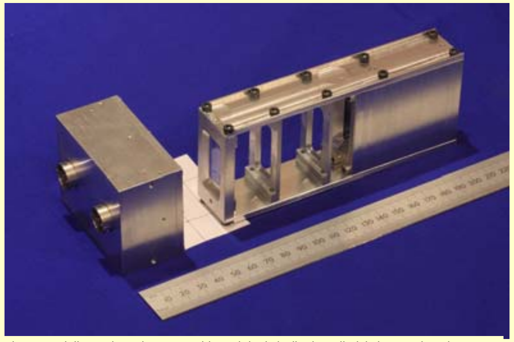

Figure 4. Violin-Mode emitter assembly and dual- (split-photodiode) detector housing.

Figure 5. Component parts for the 4 emitters and 2 dual detectors of the VM detection system.

Electronics

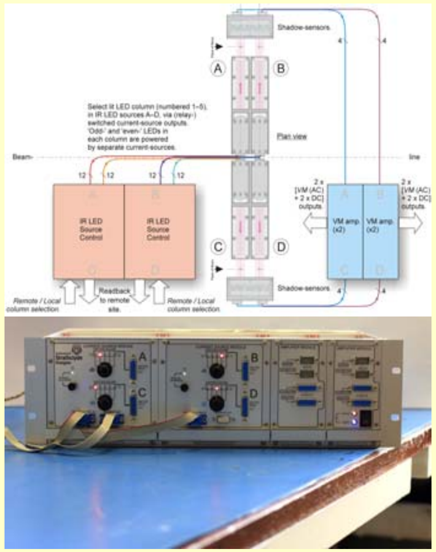

Figure 6. Low-noise current-sources and VM detection amplifiers (for a 19" rack).

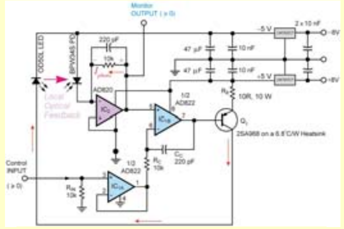

Figure 7. Infrared beam control and modulation system.

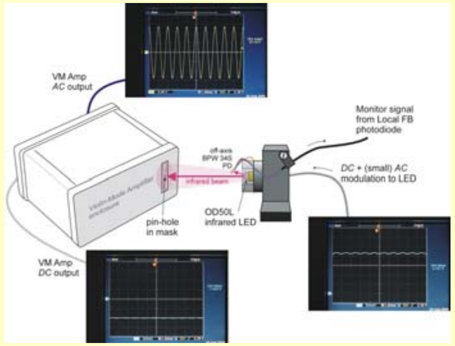

Figure 8. Measurement of *DC* and *AC* inputs and outputs of VM amplifier (modulation input was 58.0 mV p-p).

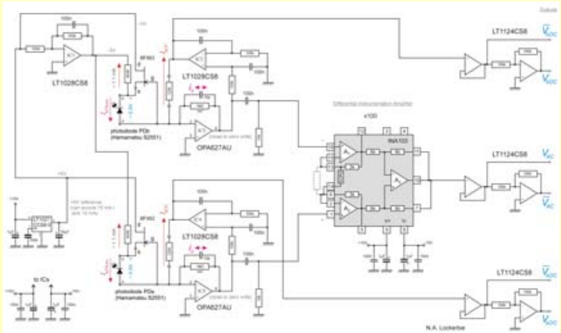

Figure 9. VM amplifier's circuit diagram, using a bootstrapped FET to remove *AC* modulation across the photodiodes PDa and PDb (in order to avoid noise-peaking, due to the self- and cable capacitance of the photodiodes).

Results

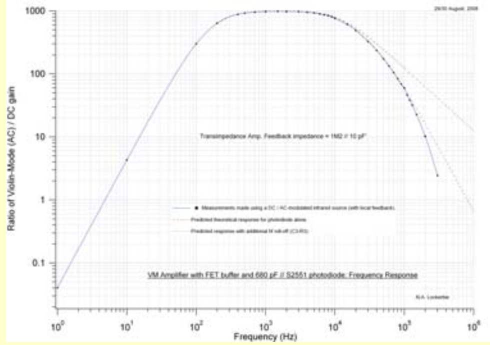

Figure 10. Measured ratio of the *AC/DC* gains of the VM amplifier, with a 680 pF capacitor in parallel with the detector's photodiode (to simulate cable capacitance). The -3dB bandwidth extended from 240 Hz–12.6 kHz.

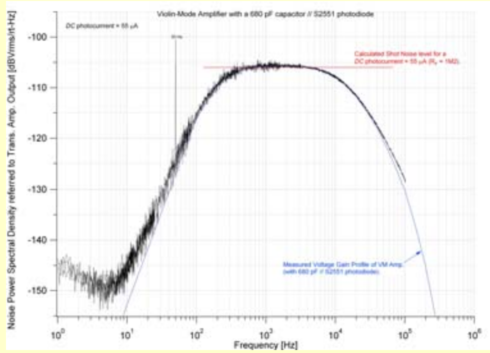

Figure 11. Power Spectral Density (PSD) of the VM amplifier, with a 680 pF capacitor in parallel with the detector's photodiode: no noise-peaking was seen.

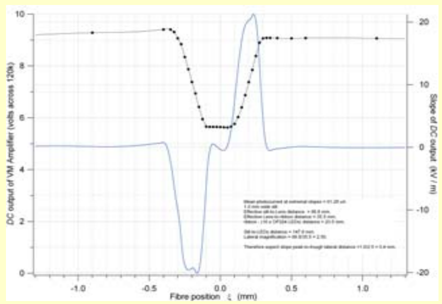

Figure 12. *DC* displacement sensitivity of the shadow-sensor, with an additional x2.5 lens acting as an optical lever (not to be used in the final application). Without this lens the displacement sensitivity would be 8 (rather than 20) kV/m.

Conclusions

In its passband the Power Spectral Density at the Violin-Mode amplifier's output was −105, +40 (for the x100 *AC* gain-stage), = −65 $dBV_{rms}/\sqrt{Hz}$, or 563 $\mu Vrms / \sqrt{Hz}$ with the single phototdiode detector. With a measured mid-band *AC/DC* displacement ratio of 1000, the *AC* rms displacement transfer function was measured to be $8 \times 10^3 \times 10^3 = 8 \times 10^6$ V_{rms}/m_{rms}, where rms values for both the displacement and the resulting *AC* voltage signal have been assumed.

And so the Violin-Mode displacement sensitvity was $(563\ \mu V_{rms} / \sqrt{Hz}) / (8 \times 10^6\ V_{rms}/m_{rms}) = 7.0 \times 10^{-11}\ m_{rms} / \sqrt{Hz}$; but, with a dual- (differential-) detector we would expect a factor $\sqrt{2}$ improvement in signal-to-noise over this figure, and so the expected displacement sensitivity becomes $7.0/(\sqrt{2}) =$ $\underline{5.0 \times 10^{-11}\ m_{rms} / \sqrt{Hz}}$.